J. of Thermal Science Vol.6, No.1

JTS

Lessons from Rotor 37

J.D. Denton

Whittle Laboratory, Cambridge University Engineering Dept., Cambridge, England

NASA rotor 37 was used as a 'blind' test case for turbomachinery CFD by the Turbomachinery Committee of the IGTI. The rotor is a transonic compressor with a tip speed of 454 m/s (1500 ft/s) and a relatively high pressure ratio of 2.1. It was tested in isolation with a circumferentially uniform inlet flow so that the flow through it should be steady apart from any effects of passage to passage geometry variation and mechanical vibration. As such it represents the simplest possible type of test for three–dimensional turbomachinery flow solvers. However, the rotor still presents a real challenge to 3D viscous flow solvers because the shock wave–boundary layer interaction is strong and the effects of viscosity are dominant in determining the flow deviation and hence the pressure ratio. Eleven 'blind' solutions were submitted and in addition a 'non–blind' solution was used to prepare for the exercise. This paper reviews the flow in the test case and the comparisons of the CFD solutions with the test data. Lessons for both the Flow Physics in transonic fans and for the application of CFD to such machines are pointed out.

Keywords: transonic compressor rotor, shock wave–boundary layer interation, CFD 'blind' solutions.

INTRODUCTION

In 1992 the turbomachinery committee of the International Gas Turbine Institute (IGTI) decided to set up a test case for CFD calculations. After some debate it was decided that the test case should be calculated 'blind', i.e. that the experimental results should not be made available until after the solutions had been submitted. NASA (Lewis Research Center) offered a suitable test case in the form of a highly loaded transonic compressor rotor which was then being tested with extensive use of laser anemometry to measure the internal flow. The measurements were supervised and the geometrical data needed for the calculations were prepared by Dr. A.J. Strazisar of NASA Lewis without whose efforts the whole exercise would not have been possible. In order to check the data test calculations were performed by J.R. Wood of NASA Lewis who had access to the experimental results and so his calculations although valuable, were not 'blind'.

Received 1996.

The computed results were submitted in April 1994. Eleven 'blind' solutions were submitted and the experimental results were made available to the authors only after their solutions were received. The comparison with the test data was supervised by Dr Strazisar and presented at the 1994 IGTI Gas Turbine Conference in June. Authors were able to repeat their calculations in the light of the test data and were able to present both their blind 'predictions' and any subsequent 'postdicted' results at the meeting. Authors were subsequently invited to prepare a brief description of both their 'predicted' and 'postdicted' results for inclusion in an ASME publication. The present author had access to all the solutions submitted and to the authors' individual reports and is grateful to all those who took part in the exercise.

TEST CASE DETAILS

Full details of the test case geometry are available from Dr. Strazisar at NASA Lewis. A meridional view

of the flow path is shown in Fig.1. The aerodynamic design parameters are given by Reid & Moore (1978) and are summarised below.

Table 1 Aerodynamic design parameters

Number of blades	36
Tip diameter at leading edge	0.5074 m
Hub diameter at leading edge	0.3576 m
Rotational speed (corrected)	17188.7 rpm
Tip solidity	1.288
Tip clearance	0.356 mm
Tip speed	454.14 m/s
Pressure ratio	2.106
Mass flow rate (corrected)	20.19 kg/s
Blading:	Multiple Circular Arc

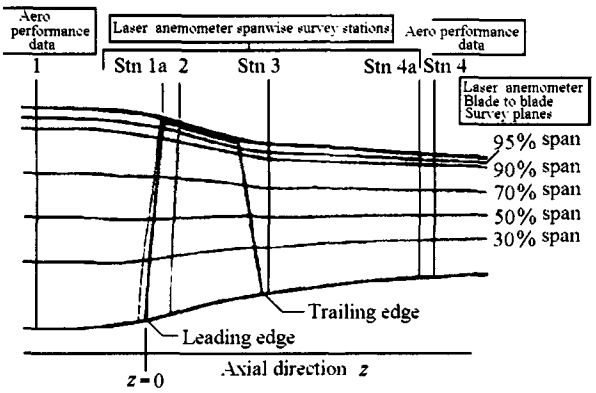

Fig.1 Rotor 37 with traverse plane locations

Table 2 Participants in the exercise and code details

AUTHOR (AFFILIATION)	NUMERICAL METHOD	GRID TYPE	TURBULENCE MODEL–WALL FUNCTIONS	NUMBER OF GRID POINTS (θ, x, r) (TOTAL NUMBER)
Arnone/Ameri (Univ. of Florence)	Explicit time marching	C	Baldwin–Lomax with W.F.	82×112×41 (376544)
Celestina. (NASA Lewis)	Explicit time marching	H	Baldwin–Lomax with W.F.	41 × 132 × 51 (276012)
Chen & Whitfield (Univ. of Mississippi)	Implicit time marching	H	Baldwin–Lomax with W.F.	41 × 131 × 51 (273921)
Chen–Naixing (Chinese Academy of Sciences)	Explicit time marching	H	Baldwin–Lomax with W.F.	25 × 71 × 21 (37275)
Chima (NASA Lewis)	Explicit time marching	H-C-O	Baldwin–Lomax No W.F.	(1057000)
Dalbert (Sulzer Turbo.)	Explicit time marching	H	Baldwin–Lomax with W.F.	33 × 99 × 33 (107811)
Dawes (Whittle Lab. Cambridge)	Explicit time marching	H	Baldwin–Lomax with W.F.	33 × 101 × 33 (109989)
Denton & Xu (Whittle Lab. Cambridge)	Explicit time marching	H	Simple mixing length with W.F.	37 × 150 × 37 (205350)
Hah (NASA Lewis)	Implicit Pressure Correction	Non–Periodic H	$k-\varepsilon$ No W.F.	58 × 151 × 51 (446658)
Paris (Northern Research)	Implicit Beam & Warming	H	Baldwin–Lomax	51 × 76 × 26 (100776)
Wiss (Sulzer Innotec)	Implicit Pressure Correction	H	$k-\varepsilon$	30 × 95 × 35 (99750)
Wood (NASA Lewis) Not Blind	Explicit time marching	H	Baldwin–Lomax with W.F.	Various

Detailed laser surveys of the flow field are available at stations 2 and 3 (Fig.1) and aerodynamic probe traverse data at stations 1 and 4. These were processed to obtain the compressor pressure ratio: mass flow and efficiency: mass flow characteristics. The inlet distributions of stagnation pressure and temperature were provided to the participants who were asked to predict the overall performance and to present predictions of the detailed flow field at points corresponding to 98% and 92.5% of their own calculated choking flow rate. Because previous studies have shown that the calculated pressure ratio and efficiency depend significantly on the method by which the flow field is averaged, it was requested that the calculated results should be averaged in the same way as the experimental data when making the comparisons of overall performance. Unfortunately very few participants bothered to do this.

In order to check for grid dependency, all authors were also asked to provide results from solutions with half their standard number of mesh points in the pitchwise direction.

Further details of the flow in the compressor are provided by Suder et al. (1994) who showed a remarkable dependence of the performance on the fine detail of the leading edge geometry and roughness, and by Suder & Celestina (1994) who studied the tip leakage flow both experimentally and computationally. Results obtained by Sulzer for this compressor have been published by Dalbert & Wiss (1995).

SOLUTIONS SUBMITTED

Details of the authors who provided solutions together with the methods and number of grid points used are given in Table 2. In fact three solutions (those of Dawes, Dalbert and Wood) were obtained with the same code, Dawes' 'BTOB3D', used by different authors and with different grids.

The computers used are listed in Table 3 together with a very rough estimate of the equivalent CRAY YMP times needed for a solution. The latter are extremely approximate because the benchmarking exercise in which participants were asked to assess the

Table 3 Computer Resources Used by the Participants

AUTHOR (AFFILIATION)	COMPUTER USED AND ITS SPEED RELATIVE TO THE CARY YMP	RUN TIME IN MICROSECONDS PER POINT PER STEP/ITERATION	NUMBER OF STEPS/ITERATIONS PER SOLUTION AND OF GRID POINTS	EQUIVALENT CRAY YMP RUN TIME HOURS
Arnone/Ameri	CRAY YMP	55	200 Cycles	1.17
(Univ. of Florence)	1		376544	
Celestina.	CRAY C90	13	4500	12.6
(NASA Lewis)	2.8		276012	
Chen & Whitfield	CRAY C90	33	4200	29.5
(Univ. of Mississippi)	2.8		273921	
Chen Naixing (Chinese	486 PC 66 MHz.	3200	3600	3.5
Academy of Sciences)	0.03		37275	
Chima)	CRAY C90	7.02	2000	11.5
(NASA Lewis)	2.8		1057318	
Dalbert	SG Iris	233	2500	1.92
(Sulzer Turbo.)	0.11		107811	
Dawes (Whittle	IBM RS6000 380	130	4500	3.6
Lab Cambridge)	0.2		109989	
Denton & Xu (Whittle	IBM RS6000 350	36	5000	1.23
Lab, Cambridge)	0.12		205350	
Hah	CRAY YMP	25	650	2.0
(NASA Lewis)	1		446658	
Paris	HP 735	176	6000	7.1
(Northern Research)	0.24		100776	
Wiss	IBM RS6000 350	5000	300	8.3
(Sulzer Innotec)	0.2		99750	

speed of their computers was not very successful. The benchmark program provided would not run on some machines and was modified or run without optimisation by some participants. The times in the final column take no account of the number of grid points used, or of the quality of solution, or of the convergence tolerance achieved and so should not be treated as a measure of the efficiency of the codes. In fact it was surprising that the convergence of most codes on the test case was not good and authors tended to measure convergence subjectively in terms of constancy of global parameters, such as mass flow and pressure ratio, rather than in terms of the average or maximum residuals. It may be that the failure to achieve low residuals was due to some unsteadiness in the real flow. Although only one of the codes was run in an unsteady mode (Chen & Whitfield) it is common experience that time dependent codes will not stabilise when the real flow is unsteady.

Comparing the methods and computer resources in these tables it is apparent that the number of grid points used by the participants has been chosen to match the computer resources available with as few as 40000 points being used on a PC, typically 100000 to 200000 points on a workstation and up to 1 million points on a super computer. The number of points needed to obtain an acceptable solution is an important question that this exercise should try to answer.

COMPARISON OF OVERALL PERFORMANCE

The overall aerodynamic performance of Rotor 37 was obtained by weighting the traverse data in a manner that was carefully described to the participants who were asked to process their computed data in exactly the same manner. Unfortunately few chose to do this and most solutions were presented as mass weighted total pressure and efficiency based on data at all grid points. This is unfortunate because those who did process the data in the specified manner found that there is about 2% difference in the adiabatic efficiency between the two methods with the experimental weighting giving a higher efficiency because it neglects the high loss regions in the annulus boundary layers. The pressure ratio was much less affected by this difference in processing. All the following comparisons are based on the data from all grid points and so the predicted efficiencies should be about 2% below the test data.

The choking mass flow is a good measure of the accuracy of the inviscid part of the solution because the boundary layer blockage at the throat is extremely small and so the choking mass flow is determined by the geometrical throat area. The values achieved by the blind solutions are shown in Table 4. Most solutions are within +/-0.5% of the experimental value of 20.93 kg/s and it is significant that those with more grid points tend to have more accurate predictions.

Table 4 Chocking mass flow rates

AUTHOR	CALCULATED CHOKE FLOW	% ERROR
Arnone/Ameri	20.95	+0.01
Celestina	20.93	0.0
Chen	20.88	-0.24
Chen Naixing	21.25	+1.53
Chima	20.79	-0.67
Dalbert	20.66	-1.29
Dawes	20.83	-0.48
Denton/Xu	20.91	-0.01
Hah	20.93	0.0
Paris	21.00	+0.33
Wiss	20.98	+0.24
Wood	20.80	-0.62

Before comparing the overall performance it is worth seeing how errors in pressure ratio and efficiency translate into errors in more tangible quantities, i.e. in loss coefficient and deviation. Figs.2 and 3 were obtained by performing a throughflow solution on rotor 37, adjusting the blade exit angles and loss coefficient to match the measured pressure ratio and efficiency and systematically varying the loss and deviation. Fig.3 shows that a +/-2° error in deviation changes the pressure ratio by about +/-0.17 whilst Fig.2 shows that a +/-0.02 change in loss coefficient (relative to an average value of about 0.08) changes the efficiency by about +/-3%.

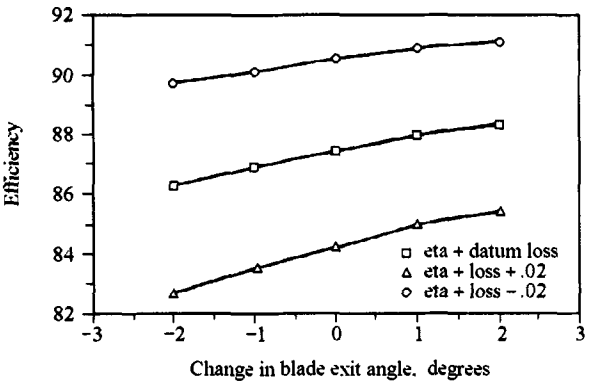

Fig.2 Effect of loss and deviation on efficiency

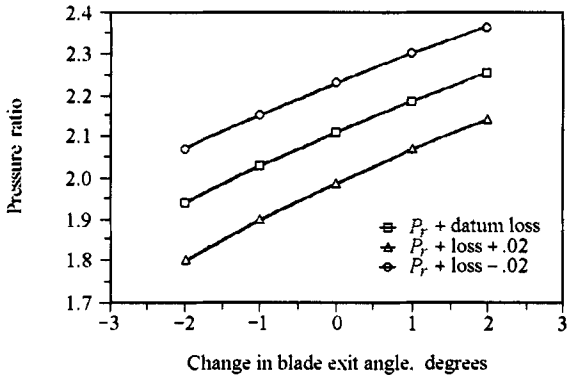

Fig.3 Effect of loss and deviation on pressure ratio

Another important factor affecting performance is the tip clearance. The measured tip clearance was about 0.40 mm but there was some uncertainty about this and the value given to participants was 0.356 mm. This corresponds to about 0.54% of leading edge span and 0.7% of trailing edge span. Only two of the methods used placed a proper grid in the tip gap. All the others used either simple periodicity across the thick blade or used the 'pinched tip' model in which the blade is artificially thinned to zero thickness in the gap where periodicity is again applied. In these methods there is no pretence of predicting the details of the flow in the tip gap but it is argued that if the leakage mass flow and momentum are correct the overall flow will be correctly captured. However, to obtain the correct leakage flow the contraction of the tip leakage jet has to be guessed and the clearance reduced accordingly. Hence most calculations used about 60% of the true gap to model the leakage flow, although authors were told that the actual tip edge was rounded by erosion and so the contraction coefficient may have been greater than this.

The effect of this uncertainty in tip clearance on the solution is illustrated in Fig.4 which shows the author's predictions for the effect of tip gap on efficiency and pressure ratio at a fixed exit static pressure. The mass flow rate also reduced significantly with increasing tip clearance. It is clear that accurate knowledge of the tip gap and contraction coefficient are essential if accurate predictions are to be obtained.

Fig.5 compares the pressure ratio: mass flow characteristic for all participants, the shaded band represents the uncertainty in the experimental data. It is clear that on average the pressure ratio is over predicted with two solutions being particularly high and one particularly low. One of the high pressure ratio solutions (Number 3 on Fig.5) was due to the present author and he was subsequently able to correct this to obtain much better agreement by reducing the upper limit on the mixing length in his code. The importance of using a blind test case is highlighted by the fact that this correction was made within 48 hours of seeing the experimental results. The other high pressure ratio solution was also subsequently corrected by the developer of the code by means of a modification to the discretisation of the viscous terms.

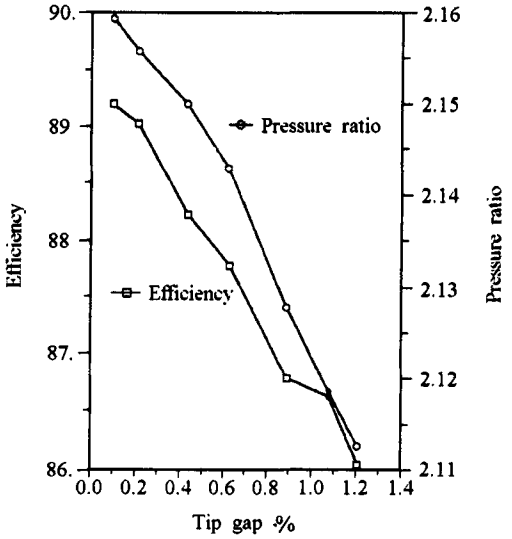

Fig.4 Calculated effect of tip clearance on pressure ratio and efficiency

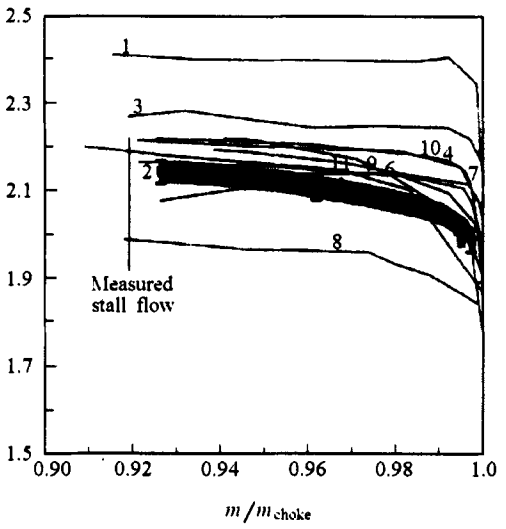

Fig.5 Measured and predicted stagnation pressure ratio

Fig.6 compares the efficiency: mass flow characteristic for all participants. The efficiency is on the whole predicted to be lower than the data but if the predictions had been processed in the same way as the experiments their level would be increased by about 2% bringing their average more into line with the data. The shape of the efficiency curve is on the whole well

predicted and the stalling mass flow is also reasonable. The latter was obtained by all participants as the point beyond which the calculation refused to converge. This point is, however, subjective as, near to stall the mass flow may drift downwards extremely slowly over many thousands of steps/iterations, even after the normal convergence criteria have been met. The author also found definite signs of hysteresis in the solution near the stall point.

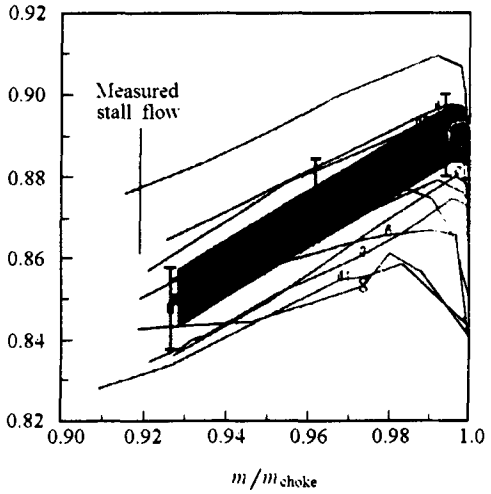

Fig.6 Computed and measured adiabatic efficiency

An interesting point about the characteristic is that the peak efficiency is reached at the choking flow rate. This is in contrast to most transonic fans with which the author is familiar where peak efficiency occurs at a few percent lower than choking mass flow. The reason for this is that near choke the shock system in the inner half of rotor 37 consists of two distinct shocks, a bow shock and a passage shock as illustrated in Fig.7. At lower mass flow rates these shocks combine to form a single strong bow shock. The fact that the compression is split between two shocks at low pressure ratios reduces the shock loss and so increases the efficiency. The reason that this occurs in rotor 37 is believed to be because the relatively thick blade sections cause a large leading edge wedge angle which in turn produces a strong bow shock. This is a desirable feature which should be encouraged in design when possible.

It is interesting to discuss why the efficiency is comparatively well predicted for this test case. This is believed to be because the flow is transonic over the whole span and so about half the total loss is shock loss which should be predicted by any flow solver irrespective of grid density. The remaining loss is due to thick separated or nearly separated boundary layers and it would be expected that its magnitude is very dependent on transition and turbulence modelling and that it would require a very large number of mesh points to resolve it accurately. However, there exists a feedback whereby if the boundary layer is predicted to be too thick the post shock Mach number is raised and the shock loss is reduced and vice–versa. Hence the resultant efficiency is little changed by errors in boundary layer thickness. This is probably the reason why reasonable solutions were obtained by methods which only placed 3 or 4 grid points within the boundary layers.

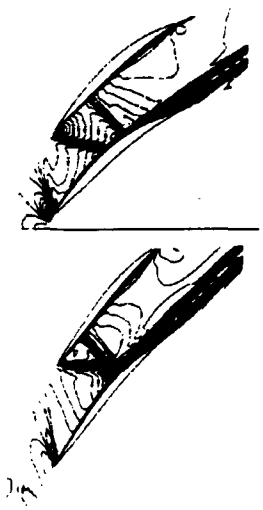

Fig.7 The shock system near hub (upper) and at mid-span (lower) at low back pressures

PREDICTIONS OF THE FLOW DETAILS

There are too many details of the flow to discuss all of them in this paper. The ones that the author found most useful as an aid to understanding the flow are to blade to blade Mach number contour plots obtained with the laser anemometer. The experimental results at mid-span and 90% span at the 98% flow condition are shown in Fig.8. At this condition there is a single bow shock at all spanwise positions. This shock is clearly detached from the leading edge at the tip and near to the hub but is very nearly attached at 50% span. The shock is not quite normal to the flow in the blade to blade surface at either location indicating that the blade can support a slightly greater pressure rise before stall. Most solutions predicted the overall shock pattern remarkably well. The shock was usually captured clearly at the leading edge with the amount of shock smearing being mainly dependent on the number of mesh points used rather than on the numerical method. However, several methods showed the shock badly smeared as it approached the suction surface. This was due to the use of too coarse a grid

in the middle of the blade whilst a fine grid was used at the leading edge and trailing edge. Since the shock is always smeared over at least 3-4 grid points it is important that these points are close together everywhere that a shock might occur. Fig.9 shows the author's solution at mid-span at three different levels of grid refinement. It is clear that the shock is sharpened and the boundary layers thinned as more grid points are used but the overall character of the solution is not changed. The author found that the overall performance was also surprisingly little affected by grid refinement but other contributors reported greater effects.

A very important feature of the Mach number contours is that the post shock Mach numbers are generally predicted to be significantly lower than measured. This is difficult to verify from the contours but is better illustrated by Fig.10 which shows the pitchwise variation of Mach number through the shock at station 2 and 50% span. Unfortunately the laser data does not extend to the suction surface but it is clear that the predicted Mach numbers agree well with the

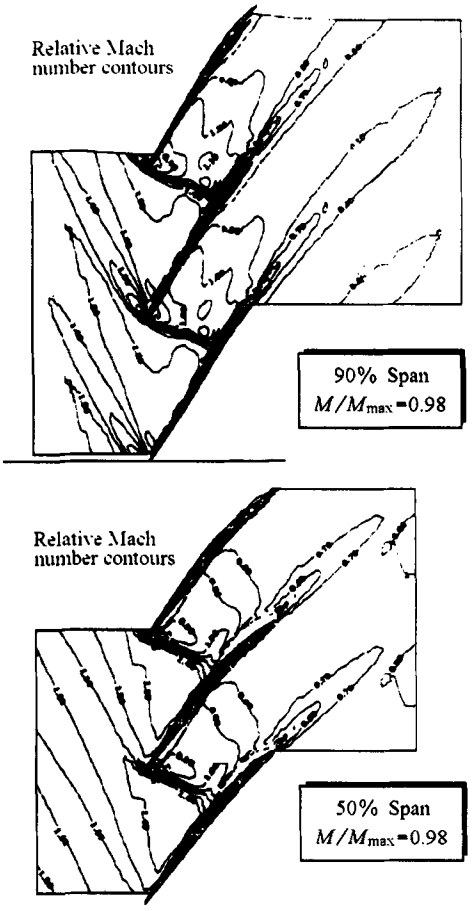

Fig.8 Measured Mach number contours at 50% and 90% span

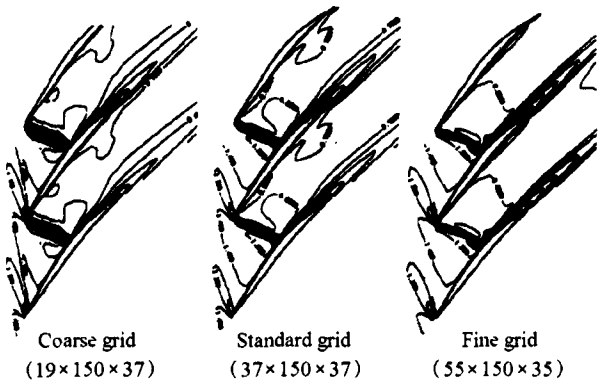

Fig.9 Computed Mach number contours at mid-span for different levels of grid refinement

measured ones in front of the shock but almost all predictions are too low after the shock. This is the key to the overprediction of pressure ratio and the most likely explanation is that the increase in boundary layer thickness during the shock–boundary layer interaction is actually greater than the predictions. Further evidence of this is provided by a plot of measured Mach number along the mid-pitch line which is given by Suder et al. (1994-1) and is reproduced in Fig.11. This shows the flow re-accelerating after the shock for about 25% of the chord before diffusing towards the trailing edge. This acceleration can only be a result of the boundary layer blockage continuing to increase for some distance downstream of the shock. Most solutions did not show this re-acceleration. The author's solutions showed it clearly but it occurred over a shorter distance close to the shock indicating that the boundary layer growth behind the shock was too rapid. In low speed flow the effects of this boundary layer growth would be confined to a region close to the suction surface but the flow behind the shock is at a Mach number of about 0.9 and so the disturbance spreads almost immediately in the cross flow direction. This acceleration and subsequent diffusion would seem to indicate the presence of a large separation bubble starting beneath the shock foot and only closing about 25% of the chord downstream of the foot. Unfortunately the laser measurements did not penetrate close enough to the suction surface to verify the presence of such a bubble. Most of the fine grid predictions certainly showed the flow separating beneath the shock but whether or not it subsequently reattached was not always clear. In the author's case it tended remain separated up to the trailing edge at around mid-span but to reattach near to the hub and tip. It is interesting that the reattachment at the tip was strongly influenced by the tip leakage flow which entrains the low momentum fluid in the separation.

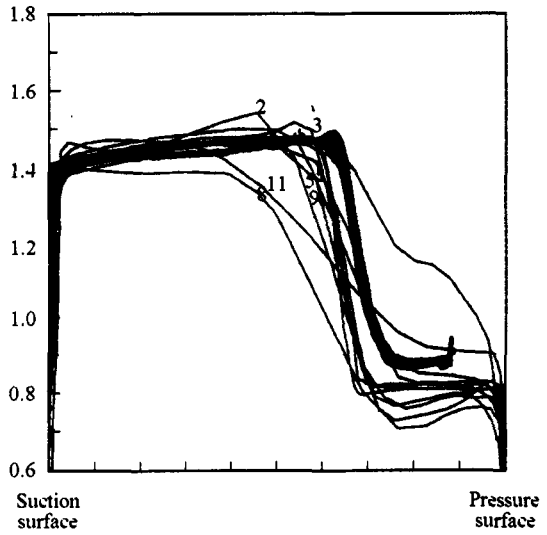

Fig.10 Measured and Computed variation of Mach number across the pitch at station 2 and mid-span

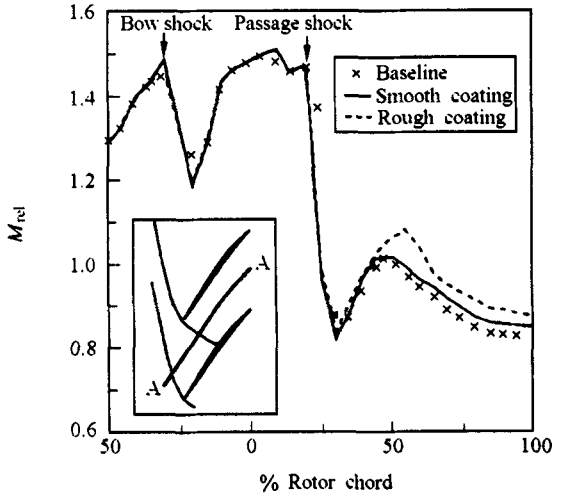

Fig.11 Measured variation of Mach number along the mid-pitch line

Another interesting feature of the separation bubble is that there was predicted to be strong radial transport of fluid from hub to tip within it. Fig.12 shows computed velocity vectors very close to the suction surface. The flow moves radially outwards immediately after the shock but reattaches over the inner half span before separating completely just upstream of the trailing edge. Beyond mid-span, however, the shock induced separation does not reattach. Such radial transport is important in moving high loss fluid from hub to tip and has the effect of increasing the apparent efficiency near the hub but decreasing it near the tip. It is most unlikely that the separation and reattachment of a flow with such strong radial transport can be predicted by conventional 2D methods. In order for the overall pressure ratio to be overpredicted it is not just necessary that the shock pressure rise should be too high, the deviation of flow at the trailing edge must also be too low. This would imply that most solutions were predicting too thin boundary layers at the trailing edge. This was certainly the case for the two solutions that predicted the highest pressure ratios in Fig.5. In both these cases the boundary layers at the trailing edge were visibly too thin due to too high values of turbulent viscosity and to incorrect discretisation of viscous terms respectively. Correcting these errors thickened the boundary layer and reduced the predicted pressure ratios. In the author's case the measured pressure ratio could still not quite be achieved because lowering the limit on mixing length (and hence the turbulent viscosity) caused gross separation and stalling before the pressure ratio dropped to the measured value. This shows how dependent the results can be on the turbulence modelling.

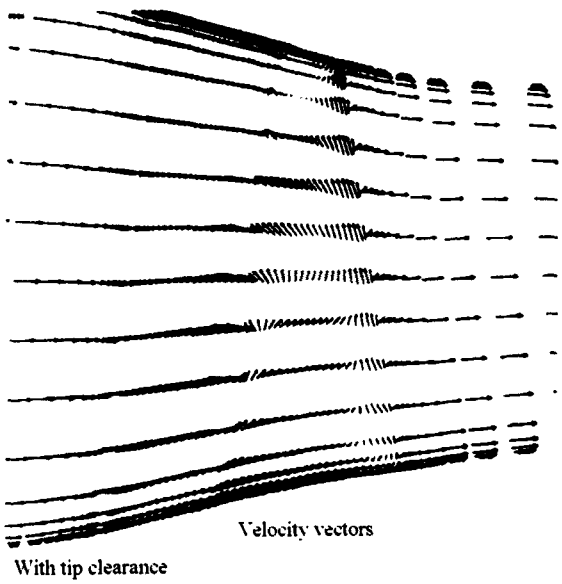

Fig.12 Computed velocity vectors close to the suction surface

The laser traverses of the wake just downstream of the trailing edge at station 2 should give some clues as to the actual boundary layer thickness at the trailing edge. Fig.13 compares the predicted and measured wake Mach number profiles at station 2 at mid-span. Although the wake widths are about correct the wake depth is clearly overpredicted by almost all participants. The underprediction of Mach number outside the wake is also apparent. The discrepancy in wake

depth is difficult to explain as it implies a considerable overprediction of boundary layer loss whereas the low post shock Mach numbers and overprediction of the pressure ratio imply an underprediction of boundary layer thickness. It may be that spanwise transport of fluid in the separated regions is moving high loss fluid towards the tip and thinning the wakes but similar discrepancies are evident in the wake depth at 90% span and the downstream traverses at station 2 (Fig.19) show no signs of a loss accumulation near the tip.

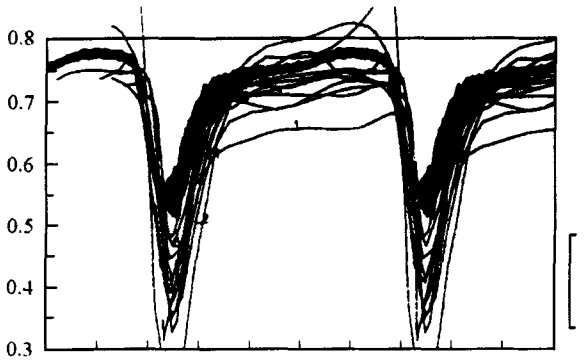

Fig.13 Computed and measured wake Mach number profiles at mid-span

The predictions of wake depth at station 4, well downstream of the trailing edge, varied greatly. In many methods the numerical smearing of the wake was so great that it was hardly recognisable by station 4, these methods tended to be those where the downstream grid was axial and not approximately aligned with the flow. However, methods which did align the grid with the flow tended to overpredict the wake depth at station 4, implying that the actual rate of wake mixing was greater than predicted. This could be because the real wake consists of an unsteady vortex street.

The measured and predicted tip leakage flow is discussed in detail by Suder & Celestina (1994-2) who show how the magnitude of the leakage effects increases towards stall. Unfortunately the laser data did not provide any results at more than 98% span and so it omitted some important details of the leakage flow. However, as shown by Fig.14, (taken from Chima's results) the effects of tip leakage on the flow at 98% span were large. The leakage flow leaves the tip gap as a jet rather than a vortex, as is shown in Fig.15. This jet 'collides' with the main flow along a lift off line extending in almost the tangential direction from the leading edge and is subsequently deflected inwards and rolls up to form a vortex which expands as it interacts with the shock. The details of this type of tip leakage flow have been discussed by Adamczyk et al. (1993). Most methods predicted this effect qualitatively but the spanwise extend of the leakage flow

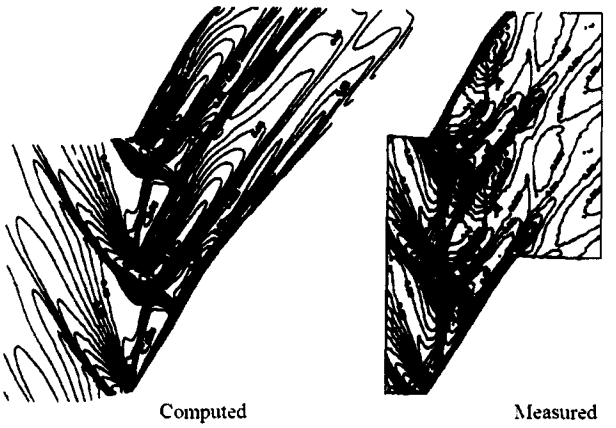

Fig.14 Measured and computed axial velocity contours at 98% span (from Chima)

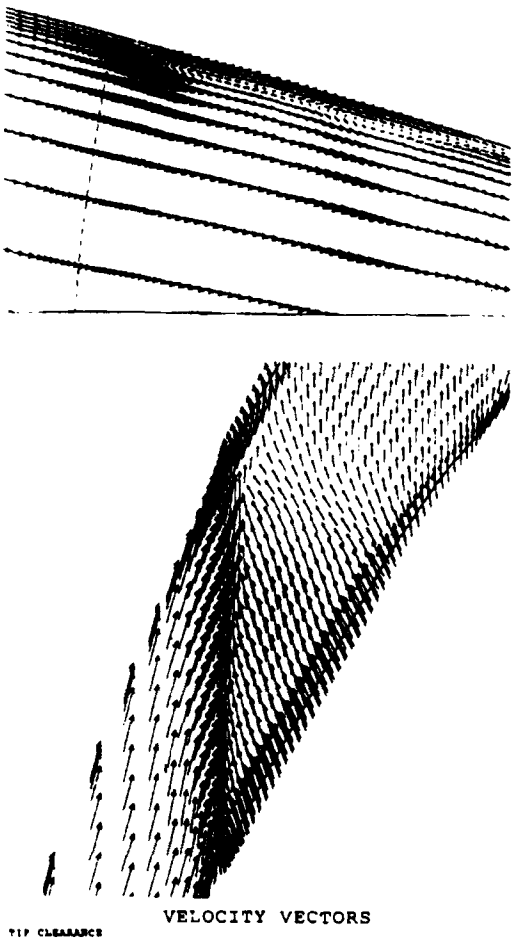

Fig.15 Velocity vectors for the tip leakage flow top-at mid-pitch bottom-very close to the casing

was underestimated by most participants. Methods which gridded the tip gap did better than those that did not but it is not possible to say whether this is simply because they used more grid points rather than because they captured the flow physics better. The reasons for the general underprediction of the leakage effects are not clear but it may be associated with an underestimate of the tip gap discharge coefficient or with the use of a slip condition on the casing. Given the important effect of tip leakage on the overall performance as shown by Fig.4 this general underestimate of leakage flow helps to explain the general overprediction of pressure ratio.

The spanwise variation of pressure ratio and temperature ratio (and hence in efficiency) downstream of the rotor are important as regards the design of downstream blade rows. Fig.16 compares the measured and predicted stagnation pressure ratios at the 98% flow point at station 4. The general overprediction of pressure ratio is apparent but the spanwise variation is also significantly different from any of the predictions. The main discrepancy is that the gradual drop of stagnation pressure from 40% span to the casing is not predicted accurately by any solution except that of Dalbert. Most of the other solutions greatly overpredict the stagnation pressure in this region. Also, no solution adequately captures the 'trough' in stagnation pressure at around 15% span, in fact only the solution by Hah (line 10 on Fig.16) shows anything like the correct trend near the hub. The discrepancies are far greater than the experimental uncertainty which is shown by the shaded region in Fig.16.

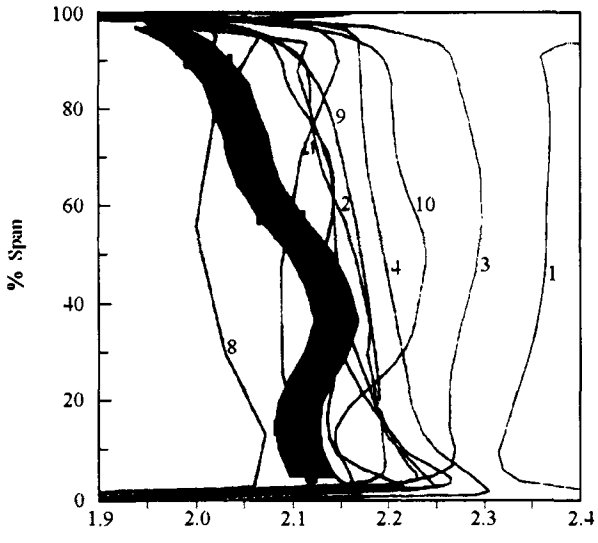

Fig.16 Computed and measured stagnation pressure ratio at station 4

Fig.17, by contrast, shows much better agreement between measured and computed efficiencies. It should be noted that these efficiencies are calculated by pitchwise mass averaging of the solutions and so are directly comparable with the experimental values. Note that the efficiency at the tip is generally predicted to be too low despite the predicted pressure ratios being too high. This is because almost all solutions predict far too high a temperature rise over the outer 15% of span. This is a major discrepancy for which the only plausible explanation for this is that the axial velocity at the trailing edge is too low in the tip region, leading to a high downstream swirl velocity.

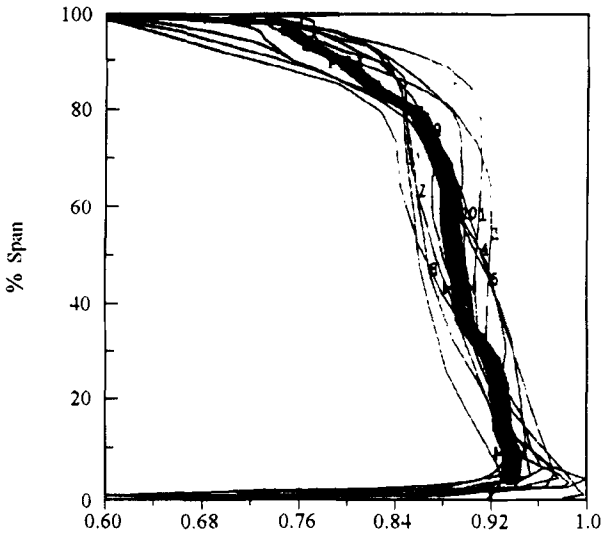

Fig.17 Computed and measured adiabatic efficiency at station 4

The agreement on efficiency is believed to be largely due to the self cancellation of errors in shock loss and boundary layer loss already discussed. The fact that the trends in efficiency variation are correct whilst the pressure variation is not implies that it is the deviation that is being wrongly predicted by the codes. In order to explain the discrepancy towards the tip the deviation would have to be about 2° greater than predicted over the outer half span and it is hard to reconcile this implication with the fact that the computed wakes are generally deeper than the measured ones in this region.

The trough in stagnation pressure at about 15% span may be due to a hub–suction surface corner separation, such separations are common in compressors and it would not be surprising if one were to occur here. The 'trough' occurred at all pressure ratios, as shown in Fig.18, although it appeared more as a

'bulge' at 40% span at low overall pressure ratios. This tends to suggest that it is not due to a corner separation which would be expected to vanish at low pressure ratios. The experimental measurements at station 3 do not penetrate close enough to the hub to resolve the question. As shown in Fig.19 they show definite signs of a thickening of the wake at the innermost measurement point, 25% span, but not enough detail is shown to say whether or not this is caused by a separation. Only Hah's solution predicted a corner separation on the hub. The author has tried to provoke such a separation by refining the grid and thickening the inlet boundary layer at the hub, but without success. Previous experience suggests that the existence of such separations is very dependent on the state of the hub boundary layer entering the compressor and if this boundary layer were laminar then a separation is very likely. It is believed that all the calculations modelled all the boundary layers as turbulent. Inlet skew in the boundary layer also has an important influence on the formation of such separation. It may be significant that Hah uses a $k-\varepsilon$ turbulence model with a low Reynolds number correction and no wall functions. Wiss also used a $k-\varepsilon$ model but his grid was so coarse that the hub boundary layer was probably not resolved and he did not model the inlet stagnation pressure gradient which would help to provoke a separation.

Thus the question of whether or not there is a hub corner separation on the rotor is, unfortunately, not resolved. If there is a separation it could explain some of the high predictions of pressure ratio (although Hah

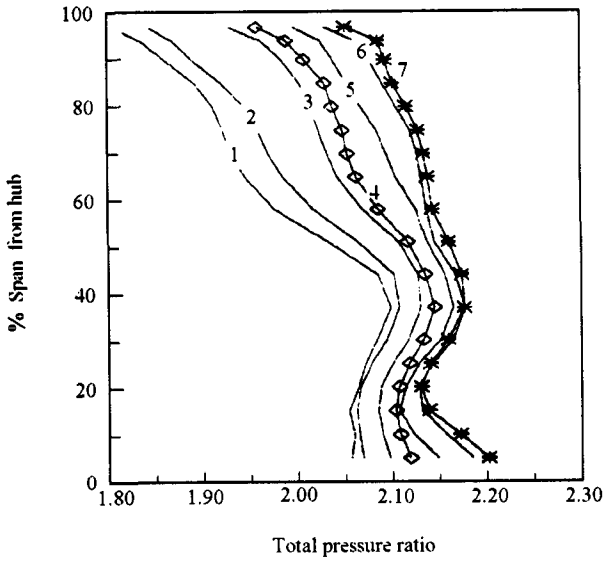

Fig.18 Measured stagnation pressure ratio at station flow for different flow rates

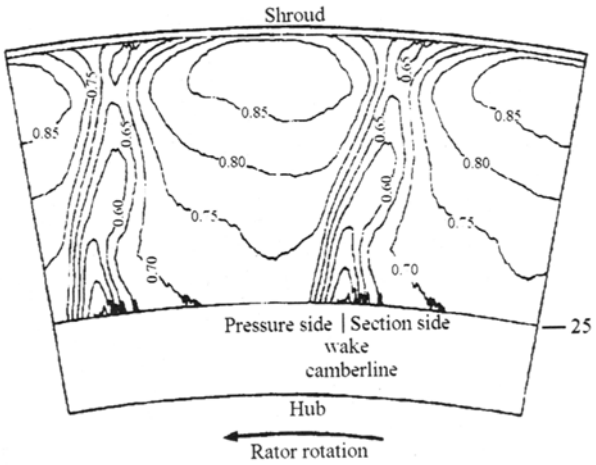

Fig.19 Relative Mach number contours at station 3, at 98% flow

obtained a higher than average pressure ratio over the remainder of the flow) and it would highlight a severe weakness in all but one of the CFD codes used. The author thinks it unlikely that a hub separation could greatly affect the flow near the casing and so a high deviation near the casing is still needed to explain the drop in stagnation pressure towards the tip. It may be that the latter is caused by spanwise movement of fluid in the separated regions on the suction surface which thins the trailing edge boundary layer at mid-span and increases it near the tip. However, Fig.19 shows no sign of a high loss region near the tip, apart from that due to the effects of tip leakage flow.

LESSONS FOR CFD

It is surprisingly difficult to draw firm conclusions for future applications of CFD to turbomachinery blade rows. The main message must be that current CFD can resolve the flow field qualitatively but the accuracy of quantitative predictions is limited to about +/-0.1 on pressure ratio and +/-2% on efficiency for this type of blade row.

In terms of code efficiency there is no evidence that implicit methods are overall any faster than the simpler explicit methods, nor that pressure correction methods are any different from time marching methods. Convergence of the codes was surprisingly difficult to achieve in terms of the average or maximum residuals and was usually based on the subjective judgement of the user.

The choking mass flow can be predicted to about +/-0.25% if sufficient grid points are used. It is sug-

gested that at least 200000 points are necessary for this. A similar number is necessary to adequately resolve the shock at all chordwise positions. A common failure was to refine the grid around the leading and trailing edges to such an extent that it was too coarse to resolve the shock around mid-chord. The author believes that the trailing edge refinement is unnecessary and may even be harmful and so more points could have been used at mid-chord without increasing the total number. There is evidence that aligning the grid with the flow downstream of the blade reduces wake smearing, which is excessive if this is not done.

Because no boundary layer measurements were available it is not possible to say how many grid points are needed to resolve the boundary layer on such blades. Most codes used wall functions with only about 5 grid points in the boundary layers, it is unlikely that this is sufficient to resolve details such as transition or separation. Nevertheless the boundary layer thicknesses predicted by most codes did seem realistic.

It has been shown by Suder et al. (1994-1) that the performance of this compressor is very dependent on the fine details of the leading edge geometry and roughness, none of the codes attempted to resolve such details and most did not even grid the leading edge circle. Arnone, who did grid the leading edge circle with 10 points, later found that he obtained better agreement on overall performance with a coarser leading edge grid.

Simple models of the tip leakage flow gave qualitatively good predictions of the flow pattern. Although methods that gridded the tip gap gave more details of the flow it is not obvious that this was not simply because they used more grid points. However, most methods seemed to underestimate the spanwise extent of the leakage flow and so may have underestimated its blockage effect.

The compressor efficiency is relatively easy to predict for this case due to the negative feedback between shock loss and boundary layer loss but this is unlikely to be true of subsonic machines where the predicted efficiency is likely to be highly dependent on turbulence modelling. The stagnation pressure ratio is much more difficult to predict for this case because it does depend on the deviation at the trailing edge which in turn depends on the turbulence modelling. The test case was a particularly difficult one in that the boundary layers were either separated or on the verge of separation at the trailing edge over most of the span and so the blockage and deviation are very dependent on the turbulence and transition modelling. The author's experience is that most transonic compressors are not quite so sensitive as this one.

The prediction of the stalling point of the compressor as the point where the calculations ceased to converge seems to be surprisingly good. It is unlikely that this would be the case if the stall point were dependent on details of the turbulence modelling and it seems likely that there is some more general principle involved in determining the point where the leading edge shock wave moves into the upstream flow causing the mass flow rate to collapse.

There is very limited evidence as shown by the results from Hah near to the hub that a $k-\varepsilon$ turbulence model, with low Reynolds number corrections, is better than the Baldwin–Lomax model. However, this method does not seem to do any better in other regions of the flow and in fact is worse than most towards the tip. Until more turbulence models are tried on this test case no recommendations can be made for the best turbulence model. The author's view is that all turbulence models are grossly approximate when applied to such a complex flow field and are unable to resolve fine details of the flow without empirical tuning of their constants. Hence he believes that it is better to use a simple model and adjust as few constants as possible.

SUMMARY

The exercise of using a blind test case has been an extremely valuable one. It has shown up the limitations of current CFD in a way that a test case for which the measured data was available to the participants was unlikely to do. In retrospect the participants were asked to provide too many results from their solutions and an overall characteristic plus the details of the flow field at one test condition would have been sufficient.

It is surprisingly difficult to draw firm conclusions regarding the current capabilities and limitations of CFD for turbomachine blade rows. A broad conclusion is that the flow field can be predicted qualitatively but not quantitatively. However, in the author's view a qualitatively understanding of the flow can be more valuable to the designer than a quantitative prediction and so the usefulness of current methods should not be underestimated. Further improvements are likely to be dependent on developments in turbulence modelling which are unlikely to take place in the short term.

Acknowledgements

This paper would not have been possible without the efforts of Tony Strazisar and his colleagues at NASA Lewis, nor without the contributions of all

those who took part in calculating the 'blind' test case. The author is grateful to them and especially to Tony Strazisar for many fruitful discussions about the flow in rotor 37. No doubt other and better solutions on rotor 37 will be published in the future but none of them will have the satisfaction or feel the excitement of taking part in this 'experiment'.

REFERENCES

[1] Reid, L., & Moore, R.D., Design and Overall Performance of Four Highly–Loaded, High Speed Inlet Stages for an Advanced High–Pressure Ratio Core Compressor, NASA TP 1337, (1978).

[2] Moore, R.D. & Reid, L., Performance of Single Stage Axial flow Compressor with Rotor and Stator Aspect Ratios of 1.19 and 1.26 Respectively, and with a Design Pressure Ratio of 2.05, NASA TP 1659, (1980).

[3] Suder, K.L., Chima, R.V., Strazisar, A.J. & Roberts, W.B., The Effect of Adding Roughness and Thickness to a Transonic Axial Compressor rotor, ASME paper 94-GT-339, (1994).

[4] Suder, K.L. & Celestina, M.L. Experimental and Computational Investigation of the Tip Clearance Flow in a Transonic Axial Compressor Rotor, ASME paper 94-GT-365, (1994).

[5] Adamczyk, J.J., Celestina, M.J. & Greitzer, E.M., The Role of Tip Clearance in High Speed Fan Stall, *ASME Journal of Turbomachinery,* **115,** (1993).

[6] Dalbert, P. & Wiss, D.H., Numerical Transonic Flow Field Predictions for NASA Compressor Rotor 37, ASME paper 95-GT-326, (1995).